

Title Siphonaxanthin, a carotenoid from green algae *Codium cylindricum*, protects ob/ob mice fed on a high-fat diet against lipotoxicity by ameliorating somatic stresses and restoring anti-oxidative capacity

Author: Jiawen Zheng^a, Yuki Manabe^a, Tatsuya Sugawara^a

^aDivision of Applied Biosciences, Graduate School of Agriculture, Kyoto University, Kyoto 606-8502, Japan

Corresponding author: Tatsuya Sugawara; Tel: +81-75 753 6212; Fax: +81- 75 753 6212. E-mail: sugawara@kais.kyoto-u.ac.jp

First author: Jiawen Zheng feitianmao0715@gmail.com

Co-author: Yuki Manabe yuukim@kais.kyoto-u.ac.jp

Abbreviations

HPLC, high performance liquid chromatography

PDA, photodiode array detector

HFD, high fat diet

TAG, triacylglycerol

HDL, high density lipoprotein

NEFA, non-esterified fatty acids

AST, aspartate aminotransferase

ALT, alanine aminotransferase

H&E, hematoxylin and eosin

TBARS, thiobarbituric acid reactive substances

TBA, thiobarbituric acid

TCA, trichloroacetic acid

GSSG, glutathione disulfide

GSH, glutathione

DMSO, dimethyl sulfoxide

qRT-PCR, quantitative reverse transcription-polymerase chain reaction

SDS-PAGE, sodium dodecyl sulfate polyacrylamide gel electrophoresis

ER, endoplasmic reticulum

ERAD, endoplasmic-reticulum-associated protein degradation

NAFLD, non-alcoholic fatty liver disease

ROS, reactive oxygen species

NASH, non-alcoholic steatohepatitis

UPR, unfolded protein response

Abstract

Oxidative stress is implicated in the pathogenesis of many diseases including obesity, non-alcoholic fatty liver disease, and diabetes mellitus. Previously, we reported that siphonaxanthin, a carotenoid from green algae, elicited a potent inhibitory effect on hepatic *de novo* lipogenesis, and an anti-obesity effect in both 3T3L1 cells and KKAy mice. Thus, we hypothesized that consumption of siphonaxanthin could improve metabolic disorders including hepatic steatosis and systemic adiposity, as well as ameliorate somatic stress under obese conditions. Both the hepatocyte cell line HepG2 and a mouse model of severe obesity, produced by feeding ob/ob mice on a high-fat diet (HFD), were used to test this hypothesis. In obese mice, siphonaxanthin intake did not improve liver steatosis or systemic adiposity. However, intake did lower plasma glucose and alanine aminotransferase (ALT) levels and diminished hepatic lipid peroxidation products and antioxidant gene expression, which increased significantly in control group obese mice. Renal protein carbonyl content decreased significantly in the siphonaxanthin group, which might also indicate an ameliorated oxidative stress. Relevantly, siphonaxanthin intake restored gene expression related to antioxidant signaling, lipid β -oxidation, and endoplasmic-reticulum-associated protein degradation in the kidney, which decreased significantly in obese mice. We found that the liver and kidney respond to obesity-induced somatic stress in a divergent pattern. In addition, we confirmed that siphonaxanthin potently induced Nrf2-regulated antioxidant signaling in HepG2 cells. In conclusion, our results indicated that siphonaxanthin might protect obesity-leading somatic stress through restoration of Nrf2-regulated antioxidant signaling, and might therefore be a promising nutritional supplement.

Keywords

Obesity; Non-alcoholic fatty liver diseases; Oxidative stress; Endothelium reticulum stress;
Carotenoid.

1. Introduction

Obesity is considered a leading risk factor for many diseases which is accompanied by increasing circulating fatty acids and insulin resistance. In obesity, substantial increases in intracellular pro-oxidant influx, electrophilic stress, and mitochondrial burden occur, leading to generation of reactive oxygen species (ROS) and oxidative stress. ROS can denaturize or modify structural and functional molecules such as proteins and DNA, thus inducing dysregulation in molecular events and biological processes. ROS and oxidative stress are also intimately related to endoplasmic reticulum (ER) stress, which can act in a highly coordinated manner to induce cell apoptosis and tissue damage, as well as to exacerbate local inflammatory response [1-3]. Obesity-induced oxidative stress and ER stress can therefore further increase the risks of developing diseases such as diabetes mellitus, non-alcoholic fatty liver disease (NAFLD), renal diseases, and cardiovascular diseases in obese individuals [1, 4-6].

Nrf2 is a primary transcription factor in counteracting oxidative stress. It regulates a variety of antioxidant genes, phase II detoxifying enzymes, biotransformation enzymes, xenobiotic efflux transporters, and inflammatory factors, which form the integral antioxidant defense system [5]. This system protects tissues and organs from oxidative injury and maintains endogenous homeostasis by scavenging ROS, highly reactive intermediates or toxic substrates. Nrf2-regulated pathways have been observed to play a role in various diseases [7]. Meakin et al. reported that Nrf2^{-/-} mice developed more severe nonalcoholic steatohepatitis (NASH) with cirrhosis, than wild-type mice, when fed on a high-fat diet (HFD) [8]. Moreover, in Nrf2^{-/-} mice, a rapid onset and progression of nutritional steatohepatitis was induced by a methionine- and

choline-deficient diet [9]. In addition, ablation of Nrf2 in experimental animals was found to cause lupus-like autoimmune nephritis and to exacerbate diabetes-induced oxidative stress, inflammation, and nephropathy [10, 11]. These studies also indicate that oxidative stress is a shared etiological factor in different diseases.

To reduce somatic oxidative stress, a sustained healthy lifestyle, consisting of dietary management and routine exercise, is generally recommended. Additionally, novel functional compounds that can boost the anti-oxidative capacity of the body with improved efficacy and prolonged action could be promising in establishing therapeutic strategies for different diseases. In light of the role of Nrf2 in detoxification and the defense system, its enhancers have more recently been proposed as a new therapeutic class in combating diseases involving oxidative stresses from divergent stimuli [7]. In fact, several natural Nrf2 enhancers such as protandim (containing herbal ingredients), sulforaphane, and curcumin have been found out to be quite effective [12]. Some nutritional compounds such as flavonoids and catechins have also been reported as potent natural Nrf2 activators [13, 14].

Siphonaxanthin is a carotenoid specifically derived from green algae such as *Codium cylindricum*. It shares a common structure with other carotenoids, containing 8 isoprene molecules, and is distinguished by a C-8 carbonyl and C-19 hydroxyl groups on its main bond [15]. Previously, we have discovered that siphonaxanthin possesses moderate anti-obesity activity by inhibiting the expression of *Pparg* and *Cebpa*, both in the 3T3L1 cell line and in the obese and diabetic murine model, KK-Ay [16]. Additionally, our previous study also showed that siphonaxanthin inhibits *de novo* synthesis of triacylglycerol in hepatocytes by exerting an

antagonistic effect on the nuclear receptor LXR α , which is a master regulator of *de novo* lipogenesis [17]. Based on a previous study, we hypothesized that siphonaxanthin might ameliorate hepatic steatosis and systemic adiposity by inhibiting the expression of lipogenic genes, and could prevent oxidative stress and ER stress by inducing antioxidant signaling. To test this hypothesis, we used the leptin deficient ob/ob mice, well documented as a murine model of spontaneous obesity, and fed them a HFD to manifest both nature and nurture factors in the pathogenesis of obesity and hepatic steatosis. The HepG2 cell line was used to investigate the effect of siphonaxanthin on Nrf2-regulated antioxidant signaling. Above all, we aimed to demonstrate the potential of siphonaxanthin as a nutritional compound targeting metabolic diseases.

2. Methods and materials

2.1. Preparation of siphonaxanthin rich fraction

Siphonaxanthin was extracted from the green algae *Codium cylindricum Holmes* [18]. For the animal study, a crude lipid fraction was first obtained by extracting with acetone from freeze dried *C. cylindricum H.* powder. The crude lipid extract was then dissolved in hexane/acetone (6:4) and subjected to silica gel column chromatography. Next, the siphonaxanthin-rich fraction was prepared through a gradient elution with hexane/acetone (9:1, 8:2, 7:3, 6:4; v/v). The final siphonaxanthin-rich fraction used in the animal study was composed of 68% siphonaxanthin and 32% other lipids of which the major component was monogalactosyldiacylglycerol (Fig. 1). For cellular study, the siphonaxanthin-rich fraction was re-dissolved in methanol and further purified

by high performance liquid chromatography (HPLC) (LC-6; Shimadzu, Japan) connected to a photodiode array detector (PDA) (SPD-M20A; Shimadzu, Japan) with a purity of above 99%.

All the samples were stored at -80°C , until further use.

2.2. Animals and diets

All experimental animal protocols were approved by the Animal Experimentation Committee of Kyoto University for the care and use of experimental animals (Approve No. 29-80). Male C57BL/6JHamSlc-ob/ob mice (6 weeks) and C57BL/6JJmsSlc mice were obtained from Japan SLC. All mice were housed individually and maintained on an alternating 12-h light/dark cycle at $23\pm 1^{\circ}\text{C}$. After an acclimatization period of 5 days, the ob/ob mice were randomly divided into control and siphonaxanthin (SPX) groups (n = 6 per group), with *ad libitum* access to drinking water. The control group was fed a modified 45% HFD (D12451, Research Diets, NJ, USA) supplemented with 2.2% soybean oil (Table 1). The siphonaxanthin group was fed a modified 45% HFD supplemented with siphonaxanthin at a dosage of 0.016% (w/w) (calculated by siphonaxanthin weight equivalent) dissolved in soybean oil (2.2% of HFD weight) (Table 1). C57BL/6J mice were designated as the normal group, fed on a basal AIN93G diet (Table 1) [19]. Body weight and food intake were monitored throughout the study. After 43 days of feeding, the mice were euthanized by exsanguination under anesthesia with isoflurane, after a 12-hour fast, and blood was collected in heparinized syringes from the inferior vena cava. Organs were rapidly removed, weighed, and immediately frozen in liquid nitrogen. Liver and kidney tissues were partially stored in RNA laterTM solution (Ambion, CA, USA) at -80°C until further analyses.

2.3. Biochemical analyses

Blood plasma was separated by centrifugation at $1000 \times g$ for 15 min at 4°C and stored at -80°C until use. Plasma concentrations of glucose, triacylglycerol (TAG), free cholesterol, high density lipoprotein (HDL) cholesterol, total cholesterol, non-esterified fatty acid (NEFA), aspartate aminotransferase (AST), and alanine aminotransferase (ALT) were measured using commercially available kits (Glu C II, TG E, F-Cho E, HDL-C E, T-Cho E, NEFA, and GOT GPT C II, respectively; Wako Pure Chemical Industries, Osaka, Japan) according to the manufacturer's instructions. Plasma creatinine was measured using the commercially available kit (Creatinine Colorimetric Assay Kit, Cayman Chemical, MI, USA). TAG, total cholesterol, and NEFA concentrations in the lipid fraction prepared from the liver tissue were measured using the commercial kits mentioned above.

2.4. Histomorphology analyses

Liver tissues were fixed in 4% paraformaldehyde and then embedded in paraffin to form blocks. Slices were stained with hematoxylin and eosin (H&E) or Sirius Red to observe the lipid droplets and fibrosis in liver tissues. Liver tissue morphology was observed, and photos were taken using the fluorescence microscope BZ-9000 (Keyence, Osaka, Japan).

2.5. Hepatic and renal oxidative stress marker

Levels of malondialdehyde in liver and kidney tissues were measured by using the TBARS assay [20]. Briefly, 40 mg tissues were homogenized in 1.15% KCl aqueous solution (400 μ L) with 5% butylated hydroxytoluene methanol solution (16 μ L). Next, 400 μ L of 0.375% thiobarbituric acid (TBA)–0.25 M HCl solution and 15% trichloroacetic acid (TCA) solution were added into the tissue homogenate, respectively, and boiled in a water bath at 95°C for 15 min. The solution was then cooled and centrifuged at 10,000 \times g for 5 min under room temperature. Absorption of the supernatant at a wavelength of 535 nm was measured with a microplate reader (Molecular Devices Co., Sunnyvale, CA). Glutathione and glutathione disulfide contents in tissue homogenates were measured using a commercial kit (GSSG/GSH Quantification Kit, Dojindo Molecular Technologies, Kumamoto, Japan), according to the manufacturer's instructions. Protein carbonyl content in kidney homogenate was measured using a commercial kit (Protein Carbonyl Content Assay Kit, Sigma-Aldrich, MO, USA), per manufacturer's instructions.

2.6. Cell culture and treatment

HepG2 cells (JCRB 1054; Health Science Research Resources Bank, Osaka, Japan) were cultured in Dulbecco's modified essential medium (DMEM) containing 10% fetal bovine serum (Invitrogen, CA, USA) and antibiotics (100 unit/mL penicillin and 100 μ g/mL streptomycin, Life Technologies Corporation, NY, USA) at 37°C in a humidified atmosphere with 5% CO₂. Cells were seeded in 12-well plates at 2.5 \times 10⁵ cells/mL for real-time quantitative reverse transcription-polymerase chain reaction (qRT-PCR) analysis or in 6-well plates at 5 \times 10⁵ cells/mL for western blot. After confluence, cells were treated with vehicle or siphonaxanthin alone for a designated time period. Siphonaxanthin was dissolved in dimethyl sulfoxide (DMSO)

before adding to the culture medium, with a final DMSO concentration of 0.2%. DMSO was used as vehicle in the experiment.

2.7. Gene expression analysis using real-time quantitative reverse transcription-polymerase chain reaction

Total RNA was extracted from HepG2 cells or tissues using the sepaSol reagent (Nacalai Tesque, Kyoto, Japan) and cDNA was synthesized from RNA by using ReverTra Ace qPCR RT Master Mix (TOYOBO, Osaka, Japan) according to the manufacturer's instructions. To perform the qRT-PCR, cDNA was diluted and mixed with iQ SYBR Green Supermix (Bio-Rad Laboratories, CA, USA) containing 1 $\mu\text{mol/L}$ PCR primer (primer sequences are shown in Table 3, 4). Real-time qRT-PCR was performed using a DNA Engine Option system (Bio-Rad Laboratories) and the expression level of each gene was normalized using β -actin as an internal control.

2.8. Western blot analysis

Cells or tissue samples were homogenized in lysis buffer [20 mmol/L Tris-HCl, pH 8; 150 mmol/L NaCl, 1% Triton-X 100, protease inhibitor (cOmplete Tablets, mini EASYpack; Roche, Mannheim, Germany)]. The homogenate was centrifuged at $12,000 \times g$ at 4°C for 15 min to collect the supernatant. Protein concentration was determined using the DC protein assay kit (Bio-Rad Laboratories). Next, the proteins were separated by 12.5% SDS-PAGE and transferred to a polyvinylidene difluoride membrane. Target proteins were probed with HMOX1 or β -actin primary antibody (1:1000; Cell Signaling, MA, USA) at 4°C overnight, and then incubated with

HRP-conjugated anti-rabbit IgG secondary antibody (1:2000, Cell signaling) at room temperature for 1 h. Signals were visualized with the substrate Chemi-lumi One (Nacalai Tesque) using a LAS-3000 visualizer (Fujifilm, Tokyo, Japan). Protein expression level was normalized using β -actin as an internal control.

2.9. Quantification of liver siphonaxanthin accumulation by high performance liquid chromatography

Siphonaxanthin was extracted from the liver tissues and subjected to HPLC analysis as previously described [16]. The lipid extracts were loaded onto Sep-Pak Plus silica cartridges (Waters, MA, USA) to remove the TAG fraction, and dissolved in methanol for HPLC analysis. The peak of siphonaxanthin was further confirmed from its characteristic UV spectrum.

2.10. Statistical analyses

Data analyses were performed using the statistical program SPSS 23 for Mac. Significance was verified between groups of normally distributed data using a 1-factor ANOVA, followed by a Tukey's post hoc analysis for animal experiments and Scheffe's post hoc analysis for cultured cell experiments. Variance homogeneity was examined using Levene's test. When the variances between groups were unequal, the data were transformed to logarithms before analysis by 1-factor ANOVA. Data are represented as means \pm SEMs. Significance was defined as $P < 0.05$.

3. Results

3.1. Physiological parameters

During the experimental period, 2 mice in the control group died and 1 exhibited an obvious open wound from severe stress, and were therefore excluded from the final statistical analyses of the control group. Therefore, all the results were presented as a sample size of 6 for the normal and siphonaxanthin groups and 3 for the control group. As shown in Table 5, there was no difference in food intake between three groups while ob/ob mice had a significant increase in body, liver and adipose tissue weight compared to wild type mice (Table 5). Plasma glucose, free cholesterol, HDL-cholesterol, total cholesterol, ALT and AST increased significantly in the control group compared to the normal group. The siphonaxanthin group exhibited a decreasing tendency in plasma glucose and a significant decline in ALT level (Table 6). Moreover, both liver triacylglycerol (TAG) and cholesterol increased significantly in ob/ob mice, while no significant difference between the control and siphonaxanthin groups was observed (Table 7).

3.2. Liver histological analyses

To evaluate progression of liver pathology, liver sections from three groups were analyzed using H&E and Sirius Red staining. As shown in Fig. 2, severe hepatic steatosis without obvious fibrosis or inflammatory cell infiltration was observed in livers of ob/ob mice compared to normal mice. No difference between the control and siphonaxanthin groups was observed in relation to hepatic steatosis.

3.3. Hepatic TBARS and gene expression related to oxidative stress, ER stress, and lipid metabolism

Liver TBARS level increased significantly in control group ob/ob mice compared to the normal group, and was recovered to a normal level in the siphonaxanthin group (Fig. 3A). However, no significant changes in hepatic GSH, GSSG, and GSH/GSSG ratio were observed (Fig. 3B-D). To determine the redox state of the liver, genes related to oxidative stress (Fig. 3E), ER stress (Fig. 3F), and lipid metabolism (Fig. 3G) were evaluated. Increases in the expression of antioxidant genes including *Gsta4*, *Nqo1*, and *Gpx4* were observed in the control group, while the siphonaxanthin group showed a significant decline in *Gsta4* and *Gpx4* expressions, as well as a decreasing trend in *Nqo1* expression (Fig. 3E). Furthermore, the expression of *Atf3*, which was related to ER stress, increased significantly in the control group and was downregulated in the siphonaxanthin group (Fig. 3F). However, expression of the ER stress marker genes, *Atf6* and *Hspa5*, decreased significantly in the control group, and were not restored by siphonaxanthin intake (Fig. 3F). Expression of *Ppara* and *Ppard*, which were related to lipid β -oxidative capacity, declined significantly in both the control and siphonaxanthin groups (Fig. 3G). A significant elevation of *Srebf* and *Cd36* was also observed in the control group, whereas *Srebf* tended to decrease in the siphonaxanthin group (Fig. 3G).

3.4. Renal TBARS, protein carbonyl content, and gene expression related to oxidative stress, ER stress, and lipid metabolism

In the kidney, TBARS level showed no significant change between the three groups (Fig. 4A), however, protein carbonyl content increased significantly in the control group and was restored to a normal level in the siphonaxanthin group (Fig. 4B). No significant change was confirmed in renal GSH, GSSG, and GSH/GSSG ratio (Fig. 4C-E). To evaluate the redox state of the kidney, gene expression related to oxidative stress (Fig. 4F), ER stress (Fig. 4G), and lipid metabolism (Fig. 4H) were evaluated. Gene expression related to antioxidant signaling, including *Hmox1*, *Gclm*, and *Gclc*, displayed a significant decline in the control group compared to the normal group. Siphonaxanthin intake tended to restore the expression of *Hmox1*, *Gclm* and *Gclc* and elevated the expression of *Nqo1* significantly (Fig. 4F). Meanwhile, *Gsta4* expression tended to increase in the control group and significantly increased in the siphonaxanthin group. The expression of *Atf3* and *Hspa5*, genes related to ER stress, significantly decreased in the control group, which tended towards recovery in the siphonaxanthin group (Fig. 4G). The expression of *Ppara* and its target gene *Cpt1b*, two critical genes involved in lipid β -oxidation, was significantly elevated by siphonaxanthin intake, compared to the control group (Fig. 4H).

3.5. Hepatic and renal HMOX1 protein expression

Protein expression of HMOX1, an important target gene of Nrf2, increased in the liver, and contrastingly, significantly decreased in the kidney of the control group, compared to the normal group (Fig. 5A-D). No significant change between the control and siphonaxanthin groups was confirmed (Fig. 5A-D).

3.6. Siphonaxanthin enhanced Nrf2 protein expression and target gene expression in the HepG2 cell line

Treatment with 1.0 or 2.0 μM siphonaxanthin alone for 24 h significantly induced Nrf2 protein expression (Fig. 6A). Concomitantly, expression of *HMOX1* and *SOD2* tended to increase and *GCLC* increased significantly with 1.0 μM siphonaxanthin treatment for 6 h (Fig. 6B).

Expression of *GSTA4* and *GCLC* tended to increase with 1.0 μM siphonaxanthin treatment and increased significantly with 2.0 μM siphonaxanthin treatment for 16 h (Fig. 6C). Expression of *NQO1* also increased significantly following 2.0 μM siphonaxanthin treatment for 16 h (Fig. 6C). A similar tendency was observed in *GPX4* and *SOD2* at 2.0 μM for 16 h (Fig. 6C).

3.7. Siphonaxanthin accumulation in liver tissue

Siphonaxanthin accumulation in liver was measured by HPLC-PDA (Fig. 7). Peaks 1-3 refer to the metabolites of siphonaxanthin, while peak 4 refers to siphonaxanthin. In the liver, 277 ± 7 ng of siphonaxanthin and 3428 ± 210 ng of metabolites per gram were detected.

4. Discussion

In the present study, we investigated the effect of siphonaxanthin on metabolic disorders and systemic stress under obese conditions in murine mouse model manifesting of both obesity and NAFLD. Siphonaxanthin mitigated liver damage and hepatic oxidative stress in ob/ob mice, as seen by the significant decline in plasma ALT level and TBARS content respectively.

Previously, Feng et al. reported that long chain fatty acids could induce antioxidant signaling in the Hepa1-6 cell line [21]. Moreover, Malaguarnera et al. reported that the induction of hepatic HMOX1 protein was an adaptive response against oxidative damage elicited by lipid peroxidation in human NASH progression [22]. In light of the above reports, the significant increase of antioxidant gene expression and HMOX1 protein expression in the liver of the control group mice in this study might indicate an antioxidant response stimulated by increased lipid peroxidation, which was mitigated in the siphonaxanthin group. Therefore, siphonaxanthin probably relieved hepatic oxidative stress and elicited the hepatoprotective effect through scavenging of reactive intermediates in the liver, rather than reinforcing antioxidant signaling. Besides, hepatic content of GSSG and GSH did not show significant changes between 3 groups, which was consistent with the gene expression results of *Gclc* and *Gclm*. Siphonaxanthin did not restore the expression of *Ppara* and *Ppard* in the liver, both of which are associated with lipid β -oxidative capacity, and this might indicate an overwhelmed oxidative capacity resulted from lipid overload in the liver.

The protein carbonylation content in the kidney, a marker for oxidative stress, exhibited a significant increase in the control group compared to the normal group and was restored by siphonaxanthin. Meanwhile, siphonaxanthin rescued the expression of some antioxidant genes which decreased in the control group, and might indicate a recovery of Nrf2 signaling in siphonaxanthin group. The decline of HMOX1 protein expression in control group agreed with the decrease of antioxidant gene expressions. In addition, unfolded protein response (UPR) signaling was dysregulated in the control group with significant decreases of *Atf3* and *Hspa5* expression, and was restored in the siphonaxanthin group. Given that *Hspa5* encodes the main

protein chaperone GRP78, which helps assemble proteins and degrade misfolded proteins in the ER, and *Atf3* encodes a transcriptional factor, which promotes cell survival under ER stress, their normal expression is indispensable for cells to survive ER stress and cell apoptosis [1, 2, 23-25]. Collectively, despite prevailing oxidative stress under hyperlipidemic and hyperglycemic conditions, the downregulation of Nrf2 and UPR signaling in the control group suggested a hyporesponsive defense system in the kidney of ob/ob mice, which was similar to the results observed in some chronic kidney disease models reporting a failed response of the Nrf2 and UPR pathway even under strong oxidative stress [32, 33]. The elevated expression of *Ppara* and *Cpt1b* gene in the siphonaxanthin group compared to control group might suggest the recovery of renal lipid β -oxidative capacity conjugated to restored antioxidant signaling.

Notably, we observed that the expression of antioxidant genes, ER stress-related genes and the HMOX1 protein exhibited discrepancies between the liver and kidney, and the two organs responded to obesity-induced somatic stress in disparate manners. While liver had an inducible Nrf2 signaling, kidney seemed to have a more severe insult and defect in the redox signaling. Such severe decline in both mRNA and protein levels of antioxidant gene expression was also reported in murine models of slowly progressive polycystic kidney disease by Maser et al. [26]. This result might reflect a possibility that tissue-specific signaling pathways might exist under chronic somatic stress. Regardless of these discrepancies, siphonaxanthin seemed to exert a favorable effect on restoring the redox homeostasis in both the liver and kidney, and this protective effect might lie in its ROS scavenging property and Nrf2 inducing capacity. Indeed, we confirmed the potency of purified siphonaxanthin on inducing Nrf2 signaling in cultured HepG2 cells [7, 27]. Intriguingly, by the end of the experiment, 2 mice in the control group had

died and 1 exhibited an obvious open wound, while no obvious abnormality was observed in the siphonaxanthin group. This result suggested that siphonaxanthin might be able to extend life expectancy by alleviating systemic stress.

Nevertheless, several contradictions between the results and our hypothesis were observed in this study. Firstly, we expected to observe the development of steatohepatitis by feeding ob/ob mice with HFD based on some previous study [28-30]. However, liver tissue analysis showed only simple fatty liver, absent in fibrosis and immune cell infiltration. As Imajo et al. reported previously that the deficiency of leptin signaling could hamper the progression to steatohepatitis, this might explain the absence of steatohepatitis in ob/ob mice in our study [31]. Secondly, siphonaxanthin failed to improve the physiological lipid profile, systemic adiposity, and hepatic steatosis, regardless of its inhibitory effect on lipogenesis or adipogenesis under the regulation of LXR α , PPAR γ and CEBP α in our previous reports [16, 17]. However, the strong suppressive effect of siphonaxanthin on either LXR α activation or PPAR γ and CEBP α expressions was confined to cell line study, and showed dosage-dependent efficacy. As the concentration of siphonaxanthin used in cell line study was much higher than in vivo study, its suppressive effect on the animal model of obesity was quite limited [16]. In addition, siphonaxanthin was supposed to compete with excessive body of endogenous ligands to downregulate the lipogenic program in the present study. Also, no direct evidence had shown that siphonaxanthin was effective in blocking the uptake of dietary lipids, which was the main source where the body fat in ob/ob mice derived from. Therefore, the failed rescue of systemic adiposity in ob/ob mice fed a HFD might be due to the low supplementary dosage of siphonaxanthin and the severe obese state. Thirdly, although the renal *Gclc* and *Gclm* expressions decreased significantly in control group

and tended to increase in siphonaxanthin group, the GSH and GSSG concentration did not show any difference among the three groups in the kidney. This result could be possible as the intrarenal glutathione was determined by three independent processes including GSH uptake, degradation and resynthesis. Since hepatic GSH content remained intact in this study, kidney might uptake the circulating GSH, mainly secreted by liver in a large amount, to compensate its declined synthesis ability and to retain the intracellular GSH/GSSG concentration [32, 33]. However, the mRNA expression might chronically receive a negative modulation signal under somatic stress.

Overall, the results suggested that siphonaxanthin could protect against liver damage, ameliorate oxidative stress, consolidate the antioxidant defense system and restore ER homeostasis at a low dosage. Still, there were several limitations about this study that need to be addressed. Firstly, we confirmed that siphonaxanthin could directly induce Nrf2 expression in hepatocyte cell line and that Nrf2 pathway activation was involved in the attenuation of somatic stress under obese state *in vivo*. However, how siphonaxanthin induced Nrf2 expression remained unknown. In addition, we could not exclude the possibility that other pathways were also involved in the restoration of systemic redox and ER homeostasis by siphonaxanthin. Given that oxidative stress and ER stress were considered to be multifaceted and multifactorial, transcriptomics analysis might be a powerful approach to help revealing alternative signaling receptors, transducers, and regulators that siphonaxanthin might act on to exert its function beyond Nrf2 pathway [34-36]. Secondly, we concluded in this study that liver and kidney responded to oxidative stress in different patterns in *ob/ob* mice fed a HFD. But whether such tissue-dependent response to somatic stress share any universality across different animal models

remained unknown. Moreover, the exact factors that contributed to the divergent responses in liver and kidney were not identified in this study. To elucidate the cross-tissue molecular mechanisms, metabolomics in combination with transcriptomics study might be helpful in defining the causative cues related to somatic stress under obese state, and in depicting the gene expression patterns linked to the regulation of stress responding pathways [37-39]. Finally, to evaluate the effect of siphonaxanthin on the development of steatohepatitis, other well-established in vivo models outreaching the frame of obese model might be suitable to set up a new investigation plan. The purity of siphonaxanthin sample could be another improving point that should be taken into consideration in the future experiment plan. Nevertheless, together with our previous research, we have shown the multifunctional properties of siphonaxanthin including antioxidation, anti-obesity, anti-inflammation and anti-angiogenesis, and thus propose it to be a promising candidate targeting chronic metabolic diseases [16, 40-43].

Acknowledgment

This research did not receive any specific grants from funding agencies in the public, commercial, or not-for-profit sectors. The authors declare no conflict of interest.

References

- [1] Kaufman RJ. Orchestrating the unfolded protein response in health and disease. *J Clin Invest* 2002;110:1389-98.
- [2] Hotamisligil GS. Endoplasmic reticulum stress and the inflammatory basis of metabolic disease. *Cell* 2010;140:900-17.
- [3] Cullinan SB, Diehl JA. Coordination of ER and oxidative stress signaling: the PERK/Nrf2 signaling pathway. *Int J Biochem Cell Biol* 2006;38:317-32.
- [4] Bonora E, Targher G. Increased risk of cardiovascular disease and chronic kidney disease in NAFLD. *Nat Rev Gastroenterol Hepatol* 2012;9:372-81.
- [5] Singh S, Vrishni S, Singh BK, Rahman I, Kakkar P. Nrf2-ARE stress response mechanism: a control point in oxidative stress-mediated dysfunctions and chronic inflammatory diseases. *Free Radic Res* 2010;44:1267-88.
- [6] Forbes JM, Coughlan MT, Cooper ME. Oxidative stress as a major culprit in kidney disease in diabetes. *Diabetes* 2008;57:1446-54.
- [7] Bataille AM, Manautou JE. Nrf2: a potential target for new therapeutics in liver disease. *Clin Pharmacol Ther* 2012;92:340-8.
- [8] Meakin PJ, Chowdhry S, Sharma RS, Ashford FB, Walsh SV, McCrimmon RJ, et al. Susceptibility of Nrf2-null mice to steatohepatitis and cirrhosis upon consumption of a high-fat diet is associated with oxidative stress, perturbation of the unfolded protein response, and disturbance in the expression of metabolic enzymes but not with insulin resistance. *Mol Cell Biol* 2014;34:3305-20.

- [9] Sugimoto H, Okada K, Shoda J, Warabi E, Ishige K, Ueda T, et al. Deletion of nuclear factor-E2-related factor-2 leads to rapid onset and progression of nutritional steatohepatitis in mice. *Am J Physiol Gastrointest Liver Physiol* 2010;298:G283-94.
- [10] Yoh K, Itoh K, Enomoto A, Hirayama A, Yamaguchi N, Kobayashi M, et al. Nrf2-deficient female mice develop lupus-like autoimmune nephritis. *Kidney Int* 2001;60:1343-53.
- [11] Yoh K, Hirayama A, Ishizaki K, Yamada A, Takeuchi M, Yamagishi S, et al. Hyperglycemia induces oxidative and nitrosative stress and increases renal functional impairment in Nrf2-deficient mice. *Genes Cells* 2008;13:1159-70.
- [12] Hybertson BM, Gao B, Bose SK, McCord JM, Maom. Oxidative stress in health and disease: the therapeutic potential of Nrf2 activation. *Mol Aspects Med* 2011;32:234-46.
- [13] Zhu W, Jia Q, Wang Y, Zhang Y, Xia M. The anthocyanin cyanidin-3-O-beta-glucoside, a flavonoid, increases hepatic glutathione synthesis and protects hepatocytes against reactive oxygen species during hyperglycemia: Involvement of a cAMP-PKA-dependent signaling pathway. *Free Radic Biol Med* 2012;52:314-27.
- [14] Park HJ, DiNatale DA, Chung MY, Park YK, Lee JY, Koo SI, et al. Green tea extract attenuates hepatic steatosis by decreasing adipose lipogenesis and enhancing hepatic antioxidant defenses in ob/ob mice. *J Nutr Biochem* 2011;22:393-400.
- [15] Sugawara T, Ganesan P, Li Z, Manabe Y, Hirata T. Siphonaxanthin, a green algal carotenoid, as a novel functional compound. *Mar Drugs* 2014;12:3660-8.
- [16] Li Z, Noda K, Fujita E, Manabe Y, Hirata T, Sugawara T. The green algal carotenoid siphonaxanthin inhibits adipogenesis in 3T3-L1 preadipocytes and the accumulation of lipids in white adipose tissue of KK-Ay mice. *J Nutr* 2015;145:490-8.

- [17] Zheng J, Li Z, Manabe Y, Kim M, Goto T, Kawada T, et al. Siphonaxanthin, a carotenoid from green algae, inhibits lipogenesis in hepatocytes via the suppression of liver X receptor alpha activity. *Lipids* 2018;53:41-52.
- [18] Ganesan P, Noda K, Manabe Y, Ohkubo T, Tanaka Y, Maoka T, et al. Siphonaxanthin, a marine carotenoid from green algae, effectively induces apoptosis in human leukemia (HL-60) cells. *Biochim Biophys Acta* 2011;1810:497-503.
- [19] Sundaram S, Yan L. Time-restricted feeding reduces adiposity in mice fed a high-fat diet. *Nutr Res* 2016;36:603-11.
- [20] Corongiu FP, Banni S. [30] Detection of conjugated dienes by second derivative ultraviolet spectrophotometry. *Methods enzymol* 1994;233:303-10.
- [21] Feng X, Yu W, Li X, Zhou F, Zhang W, Shen Q, et al. Apigenin, a modulator of PPARgamma, attenuates HFD-induced NAFLD by regulating hepatocyte lipid metabolism and oxidative stress via Nrf2 activation. *Biochem Pharmacol* 2017;136:136-49.
- [22] Malaguarnera L, Madeddu R, Palio E, Arena N, Malaguarnera M. Heme oxygenase-1 levels and oxidative stress-related parameters in non-alcoholic fatty liver disease patients. *J Hepatol* 2005;42:585-91.
- [23] Walter P, RJS. The unfolded protein response: from stress pathway to homeostatic regulation. *Science* 2011;334:1081-6.
- [24] Zhu Q, Wang H, Jiang B, Ni X, Jiang L, Li C, et al. Loss of ATF3 exacerbates liver damage through the activation of mTOR/p70S6K/ HIF-1alpha signaling pathway in liver inflammatory injury. *Cell Death Dis* 2018;9:910-23.
- [25] Li H, Cheng C, Liao W, Lin H, Yang R. ATF3-mediated epigenetic regulation protects against acute kidney injury. *J Am Soc Nephrol* 2010;21:1003-13.

- [26] Maser RL, Vassmer D, Magenheimer BS, Calvet JP. Oxidant stress and reduced antioxidant enzyme protection in polycystic kidney disease. *J Am Soc Nephrol* 2002;13:991-9.
- [27] Ruiz S, Pergola PE, Zager RA, Vaziri ND. Targeting the transcription factor Nrf2 to ameliorate oxidative stress and inflammation in chronic kidney disease. *Kidney Int* 2013;83:1029-41.
- [28] Carmiel-Haggai M, Cederbaum AI, Nieto NJTFJ. A high-fat diet leads to the progression of non-alcoholic fatty liver disease in obese rats. *FASEB J* 2005;19:136-8.
- [29] de Lima VM, de Oliveira CP, Sawada LY, Barbeiro HV, de Mello ES, Soriano FG, et al. Yojy hen shi ko, a novel Chinese herbal, prevents nonalcoholic steatohepatitis in ob/ob mice fed a high fat or methionine-choline-deficient diet. *Liver Int* 2007;27:227-34.
- [30] Koteish A, Mae Diehl A. Animal models of steatohepatitis. *Best Pract Res Clin Gastroenterol* 2002;16:679-90.
- [31] Imajo K, Fujita K, Yoneda M, Nozaki Y, Ogawa Y, Shinohara Y, et al. Hyperresponsivity to low-dose endotoxin during progression to nonalcoholic steatohepatitis is regulated by leptin-mediated signaling. *Cell Metab* 2012;16:44-54.
- [32] Bartoli G, Häberle D, Sies H. Glutathione efflux from perfused rat liver and its relation to glutathione uptake by the kidney. *Functions of glutathione in liver and kidney: Functions of Glutathione in Liver and Kidney*; Berlin: Heidelberg, 1978.
- [33] Hagen TM, Aw TY, Jones DP. Glutathione uptake and protection against oxidative injury in isolated kidney cells. *Kidney Int* 1988;34:74-81.
- [34] Arkan MC, Hevener AL, Greten FR, Maeda S, Li Z-W, Long JM, et al. IKK- β links inflammation to obesity-induced insulin resistance. *Nat Med* 2005;11:191-8.

- [35] Ilan Y, Maron R, Tukpah AM, Maioli TU, Murugaiyan G, Yang K, et al. Induction of regulatory T cells decreases adipose inflammation and alleviates insulin resistance in ob/ob mice. *Proc Natl Acad Sci U S A* 2010;107:9765-70
- [36] Item F, Wueest S, Lemos V, Stein S, Lucchini FC, Denzler R, et al. Fas cell surface death receptor controls hepatic lipid metabolism by regulating mitochondrial function. *Nat Commun* 2017;8:480.
- [37] Andrisic L, Dudzik D, Barbas C, Milkovic L, Grune T, Zarkovic N. Short overview on metabolomics approach to study pathophysiology of oxidative stress in cancer. *Redox Biol* 2018;14:47-58.
- [38] Whitfield PD, German AJ, Noble PJ. Metabolomics: an emerging post-genomic tool for nutrition. *Br J Nutr* 2004;92:549-55.
- [39] Hu Y, Li M, Lu Q, Weng H, Wang J, Zekavat SM, et al. A statistical framework for cross-tissue transcriptome-wide association analysis. *Nat Genet* 2019;51:568-576.
- [40] Manabe Y, Hirata T, Sugawara T. Suppressive effects of carotenoids on the antigen-induced degranulation in RBL-2H3 rat basophilic leukemia cells. *J Oleo Sci* 2014;63:291-4.
- [41] Manabe Y, Hirata T, Sugawara T. Inhibitory Effect of Carotenoids on Ligand-induced Lipid Raft Translocation of Immunoreceptors. *J Oleo Sci* 2019;68:149-58.
- [42] Ganesan P, Matsubara K, Sugawara T, Hirata T. Marine algal carotenoids inhibit angiogenesis by down-regulating FGF-2-mediated intracellular signals in vascular endothelial cells. *Mol Cell Biochem* 2013;380:1-9.
- [43] Ganesan P, Matsubara K, Ohkubo T, Tanaka Y, Noda K, Sugawara T, et al. Anti-angiogenic effect of siphonaxanthin from green alga, *Codium fragile*. *Phytomedicine* 2010;17:1140-4.

Figure legends

Fig. 1 **Siphonaxanthin rich fraction compositional analysis.** (A) Chromatogram of SPX rich fraction for the *in vivo* experiment and (B) UV spectrum of SPX. (C) Thin layer chromatography analysis of SPX rich fraction for *in vivo* experiment. PC, phosphatidylcholine; DGDG, digalactosyldiacylglycerol; MGDG, monogalactosyldiacylglycerol; OA, oleic acid; TA, triolein; C, cholesterol; SPX, siphonaxanthin.

Fig. 2 **Liver histological assessment.** (A-C) Representative photomicrographs of liver tissue sections stained with hematoxylin and eosin (H&E) and (D-F) Sirius Red from normal, control and SPX groups (n=6 for normal and SPX group, n=3 for control group). Original magnification, $\times 40$. SPX, siphonaxanthin.

Fig. 3 **Effects of siphonaxanthin on hepatic TBARS, GSH, GSSG and gene expression involved in oxidative stress, ER stress, and lipid metabolism.** (A) TBARS, (B) GSH, (C) GSSG and (D) GSH/GSSG ratio, (E) hepatic gene expression concerning oxidative stress, (F) ER stress and (G) lipid metabolism in liver samples from the normal, control and SPX group. Values are mean \pm SEM (n=6 for normal and SPX group, n=3 for control group). Values not sharing a common letter differ significantly ($p < 0.05$). SPX, siphonaxanthin; GSH, glutathione; GSSG, glutathione disulfide; ER, endoplasmic reticulum.

Fig. 4 **Effects of siphonaxanthin on renal TBARS, protein carbonyl content, GSH, GSSG and gene expression involved in oxidative stress, ER stress, and lipid metabolism.** (A) TBARS, (B)

protein carbonyl content, (C) GSH, (D) GSSG and (E) GSH/GSSG ratio, (F) renal gene expression concerning oxidative stress, (G) ER stress and (H) lipid metabolism in kidney samples from normal, control and SPX groups. Values are mean \pm SEM (n=6 for normal and SPX group, n=3 for control group). Values not sharing a common letter differ significantly (p<0.05). SPX, siphonaxanthin; GSH, glutathione; GSSG, glutathione disulfide; ER, endoplasmic reticulum.

Fig. 5 Effects of siphonaxanthin on hepatic and renal HMOX1 protein expression. (A) HMOX1 protein levels in the liver and (C) kidney from normal, control and SPX groups. The corresponding quantification results are displayed as graphs (B) and (D). Values are mean \pm SEM (n=6 for normal and SPX group, n=3 for control group). Values not sharing a common letter differ significantly (p<0.05). SPX, siphonaxanthin; HMOX1, heme oxygenase1.

Fig. 6 Effects of siphonaxanthin on Nrf2 activation and target gene expression in HepG2 cells. (A) Nrf2 protein level in HepG2 cells treated with vehicle, 1.0 or 2.0 μ M siphonaxanthin alone and the corresponding quantification results. Gene expression concerning antioxidation in HepG2 cells treated with vehicle, 1.0 or 2.0 μ M siphonaxanthin alone for (B) 6 h and (C) 16 h. Values are mean \pm SEM (n=3~4). Values not sharing a common letter differ significantly (p<0.05). p value shown in graph is compared to the normal group.

Fig. 7 Hepatic accumulation of siphonaxanthin. Chromatogram of lipid extractions from liver samples of obese mice supplemented with siphonaxanthin. Peaks 1-3 refers to metabolites and peak 4 to siphonaxanthin. SPX, siphonaxanthin.

Fig. 8 Schematic of proposed mechanism underlying the protective effect of SPX on obesity-leading somatic stress in liver and kidney.

Figure legends

Fig. 1 Siphonaxanthin rich fraction compositional analysis. (A) Chromatogram of SPX rich fraction for the *in vivo* experiment and (B) UV spectrum of SPX. (C) Thin layer chromatography analysis of SPX rich fraction for *in vivo* experiment. PC, phosphatidylcholine; DGDG, digalactosyldiacylglycerol; MGDG, monogalactosyldiacylglycerol; OA, oleic acid; TA, triolein; C, cholesterol; SPX, siphonaxanthin.

Fig. 2 Liver histological assessment. (A-C) Representative photomicrographs of liver tissue sections stained with hematoxylin and eosin (H&E) and (D-F) Sirius Red from normal, control and SPX groups (n=6 for normal and SPX group, n=3 for control group). Original magnification, $\times 40$. SPX, siphonaxanthin.

Fig. 3 Effects of siphonaxanthin on hepatic TBARS, GSH, GSSG and gene expression involved in oxidative stress, ER stress, and lipid metabolism. (A) TBARS, (B) GSH, (C) GSSG and (D) GSH/GSSG ratio, (E) hepatic gene expression concerning oxidative stress, (F) ER stress and (G) lipid metabolism in liver samples from the normal, control and SPX group. Values are mean \pm SEM (n=6 for normal and SPX group, n=3 for control group). Values not sharing a common letter differ significantly ($p < 0.05$). SPX, siphonaxanthin; GSH, glutathione; GSSG, glutathione disulfide; ER, endoplasmic reticulum.

Fig. 4 Effects of siphonaxanthin on renal TBARS, protein carbonyl content, GSH, GSSG and gene expression involved in oxidative stress, ER stress, and lipid metabolism. (A) TBARS, (B) protein carbonyl content, (C) GSH, (D) GSSG and (E) GSH/GSSG ratio, (F) renal gene expression concerning oxidative stress, (G) ER stress and (H) lipid metabolism in kidney

samples from normal, control and SPX groups. Values are mean \pm SEM (n=6 for normal and SPX group, n=3 for control group). Values not sharing a common letter differ significantly (p<0.05). SPX, siphonaxanthin; GSH, glutathione; GSSG, glutathione disulfide; ER, endoplasmic reticulum.

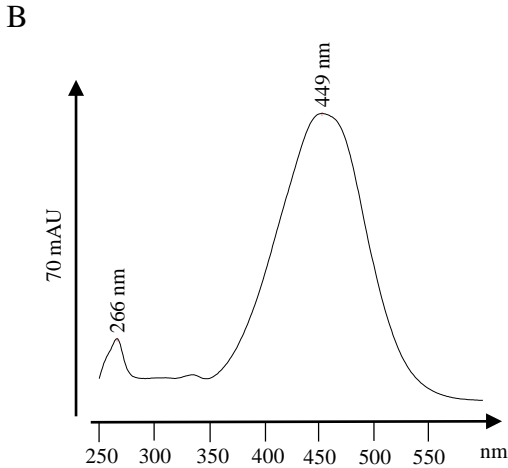
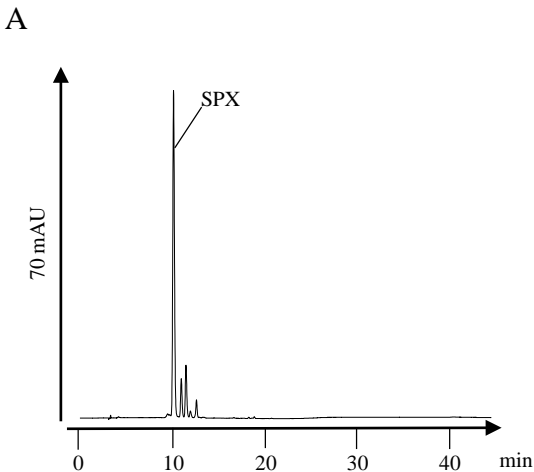
Fig. 5 Effects of siphonaxanthin on hepatic and renal HMOX1 protein expression. (A) HMOX1 protein levels in the liver and (C) kidney from normal, control and SPX groups. The corresponding quantification results are displayed as graphs (B) and (D). Values are mean \pm SEM (n=6 for normal and SPX group, n=3 for control group). Values not sharing a common letter differ significantly (p<0.05). SPX, siphonaxanthin; HMOX1, heme oxygenase1.

Fig. 6 Effects of siphonaxanthin on Nrf2 activation and target gene expression in HepG2 cells. (A) Nrf2 protein level in HepG2 cells treated with vehicle, 1.0 or 2.0 μ M siphonaxanthin alone and the corresponding quantification results. Gene expression concerning antioxidation in HepG2 cells treated with vehicle, 1.0 or 2.0 μ M siphonaxanthin alone for (B) 6 h and (C) 16 h. Values are mean \pm SEM (n=3~4). Values not sharing a common letter differ significantly (p<0.05). p value shown in graph is compared to the normal group.

Fig. 7 Hepatic accumulation of siphonaxanthin. Chromatogram of lipid extractions from liver samples of obese mice supplemented with siphonaxanthin. Peaks 1-3 refers to metabolites and peak 4 to siphonaxanthin. SPX, siphonaxanthin.

Fig. 8 Schematic of proposed mechanism underlying the protective effect of SPX on obesity-leading somatic stress in liver and kidney.

Fig. 1



C

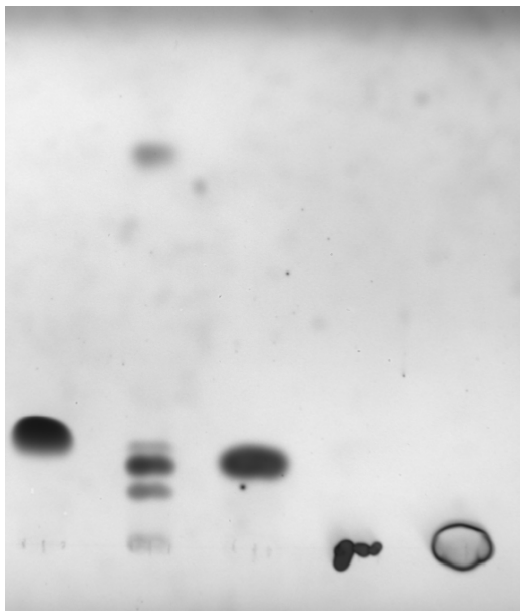
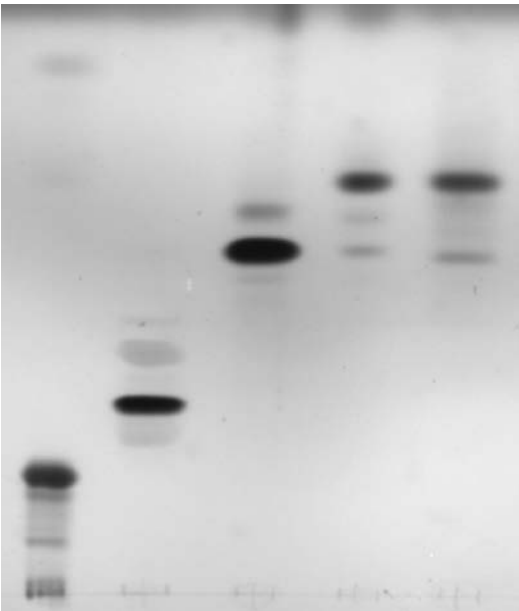


Fig. 2

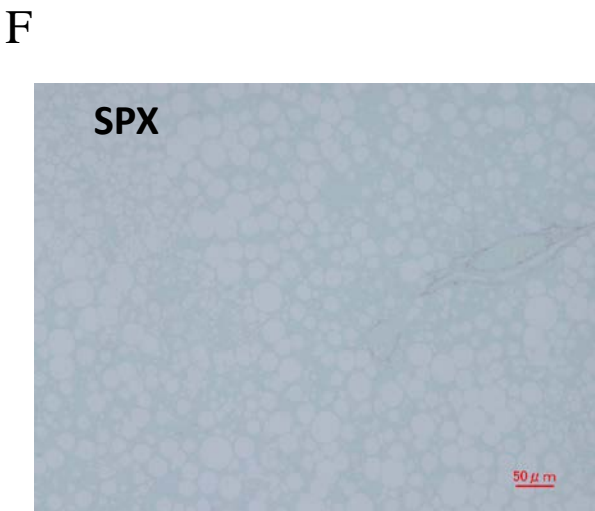
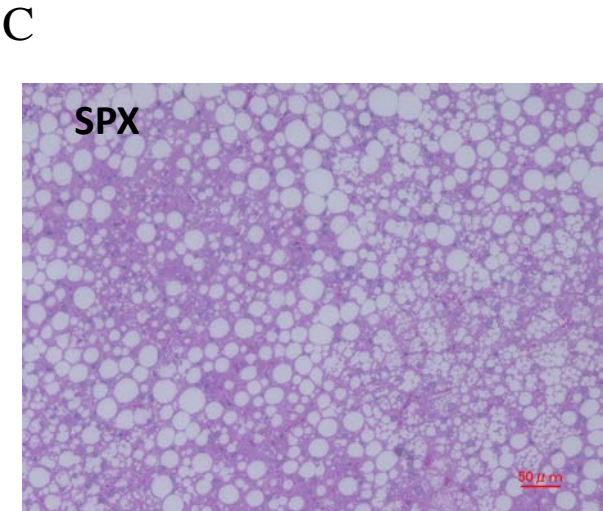
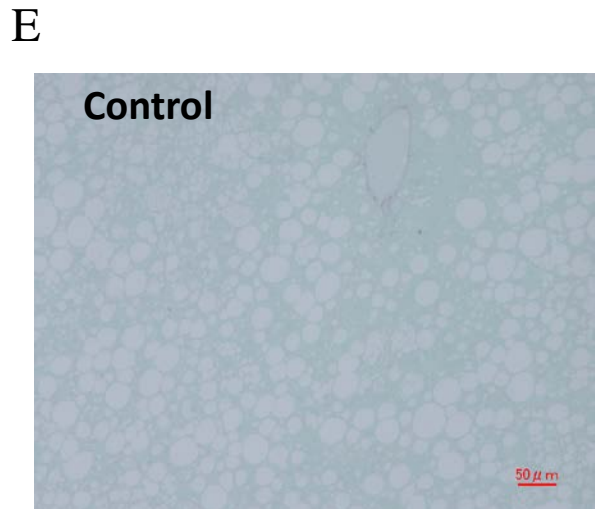
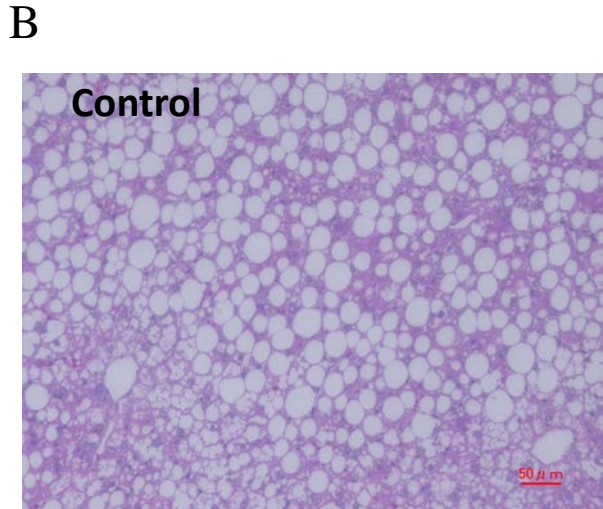
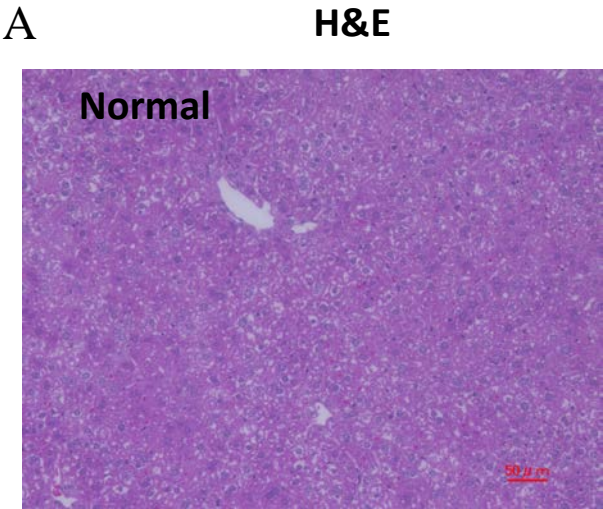
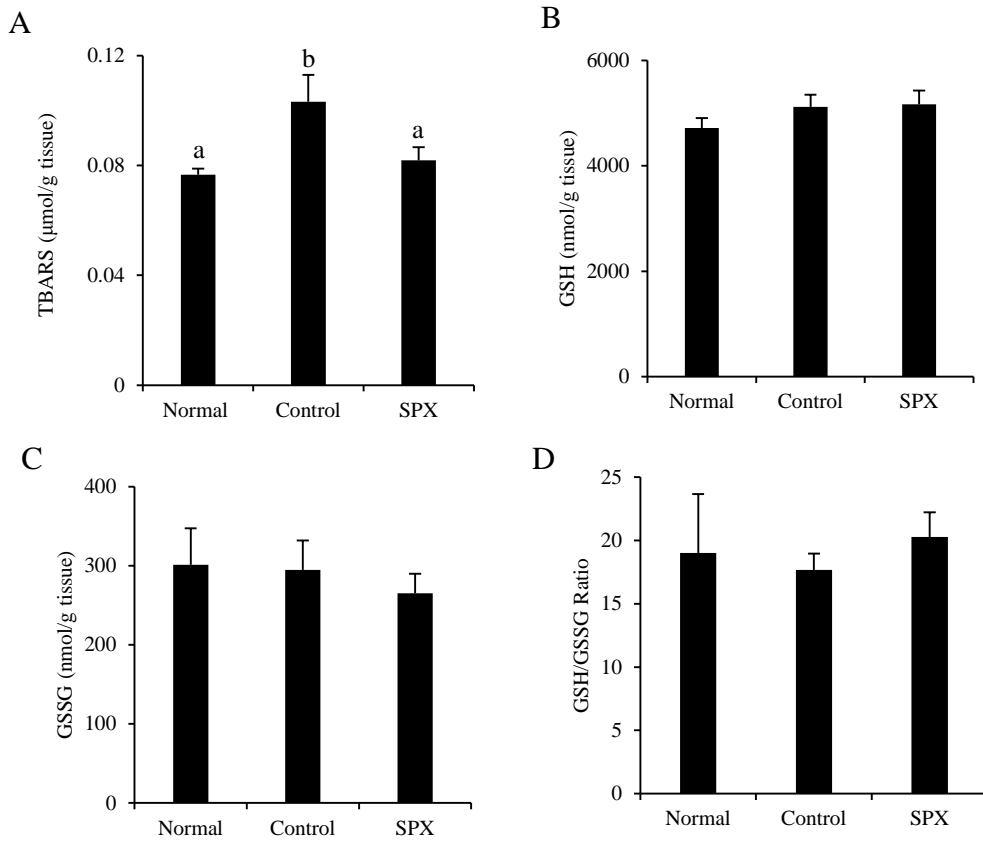
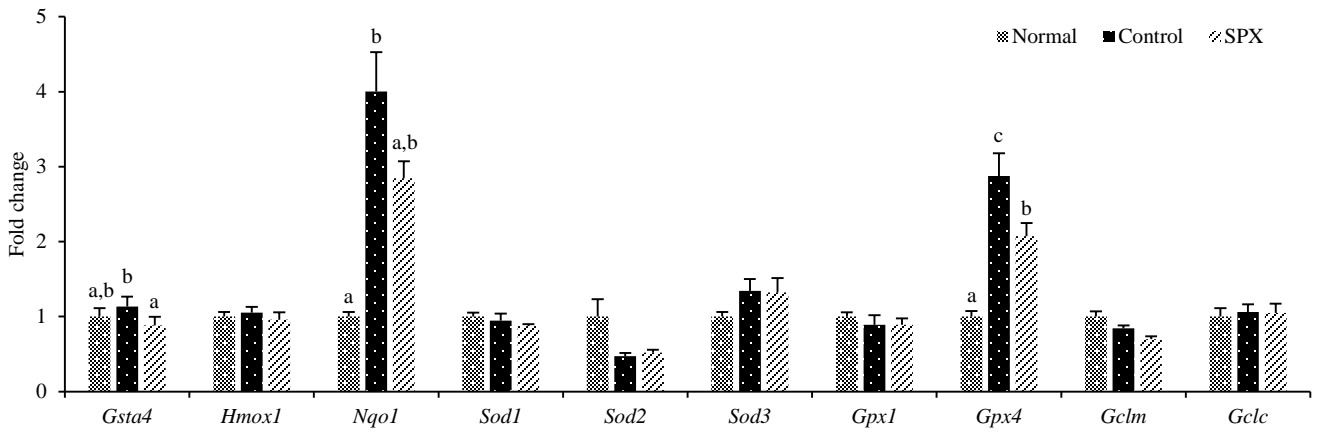


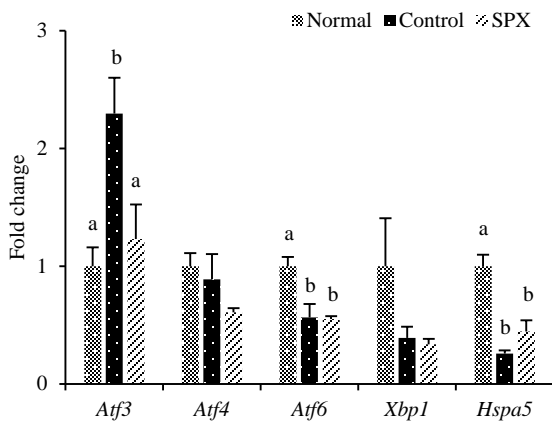
Fig. 3



E



F



G

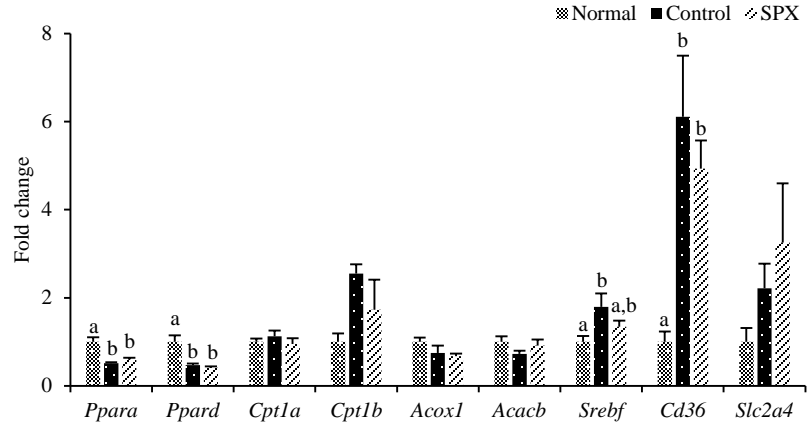


Fig. 4

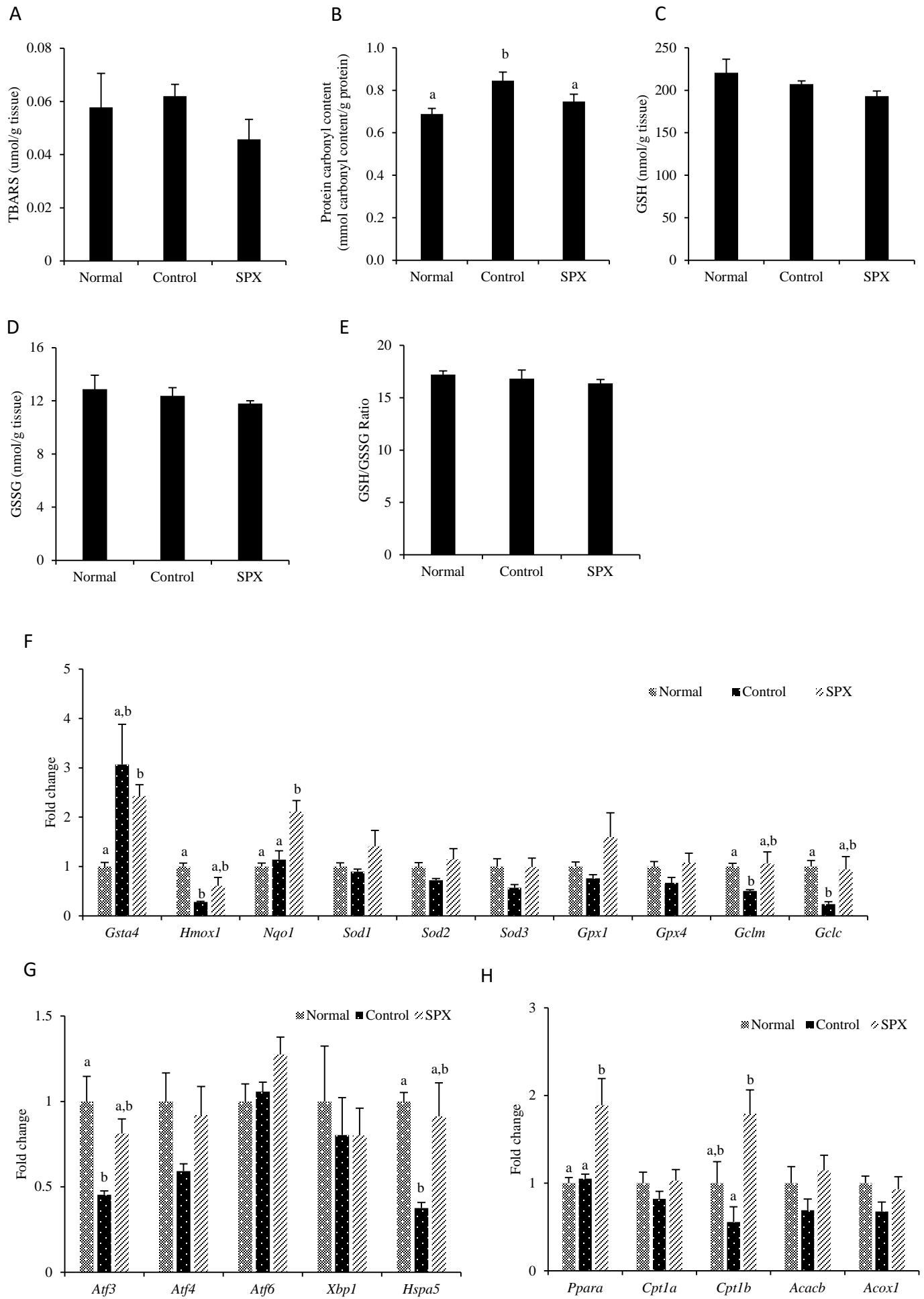


Fig. 5

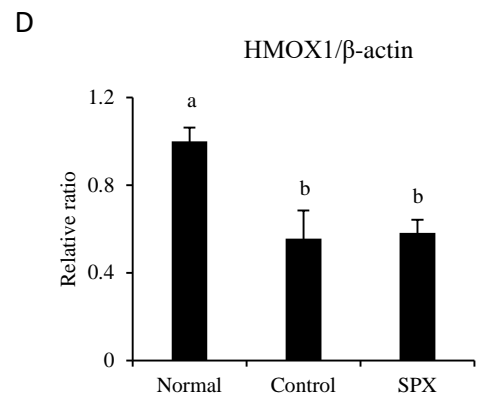
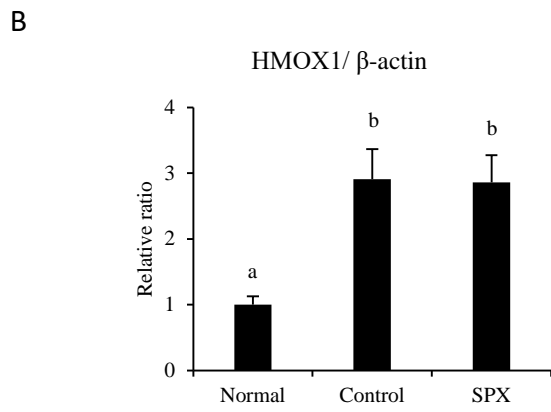
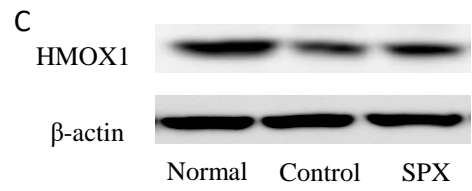
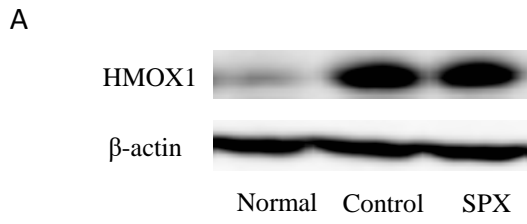


Fig. 6

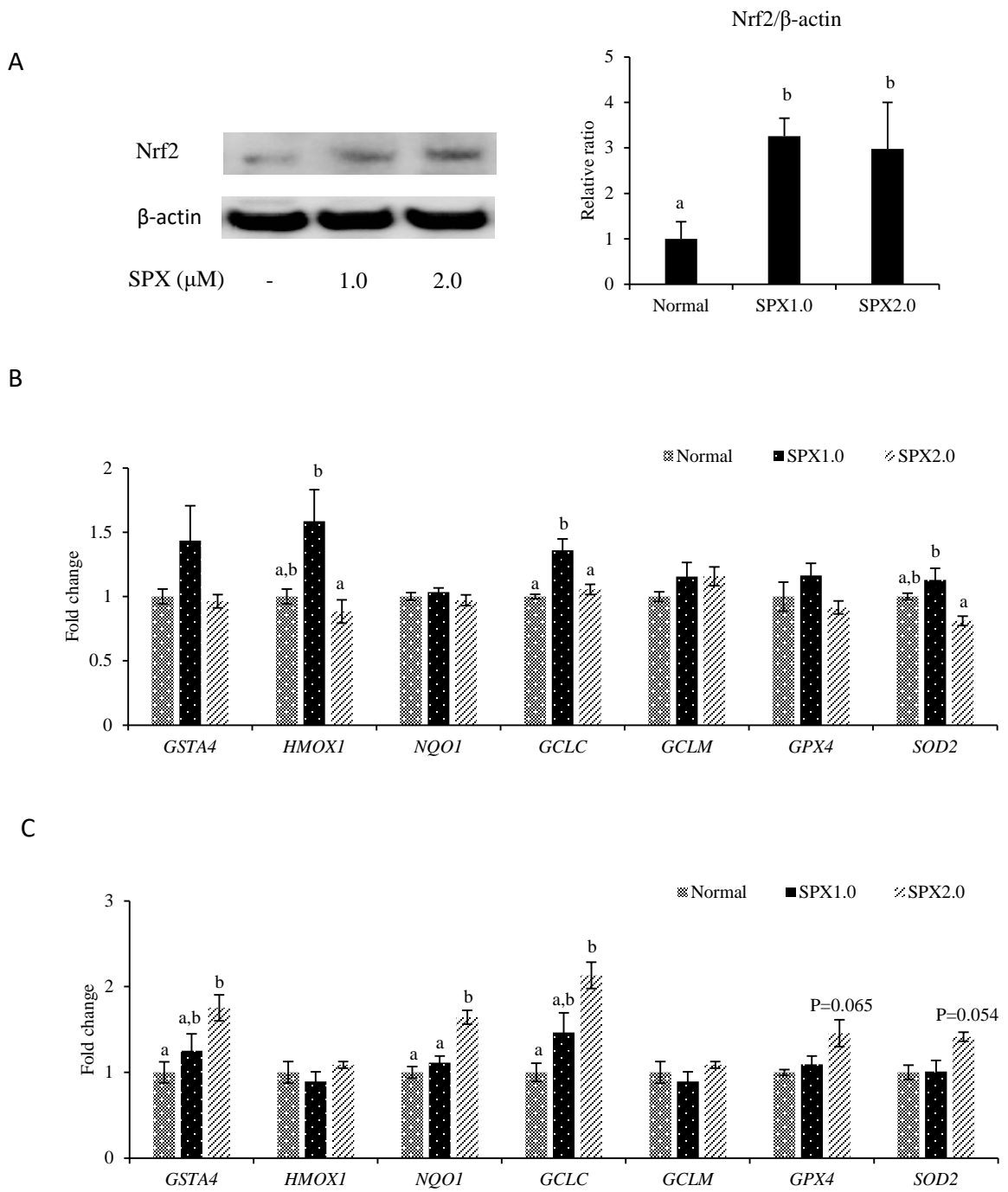


Fig. 7

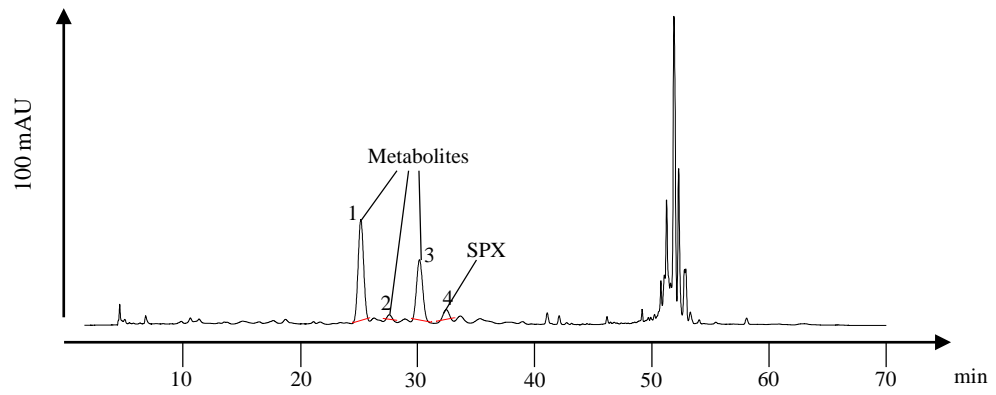
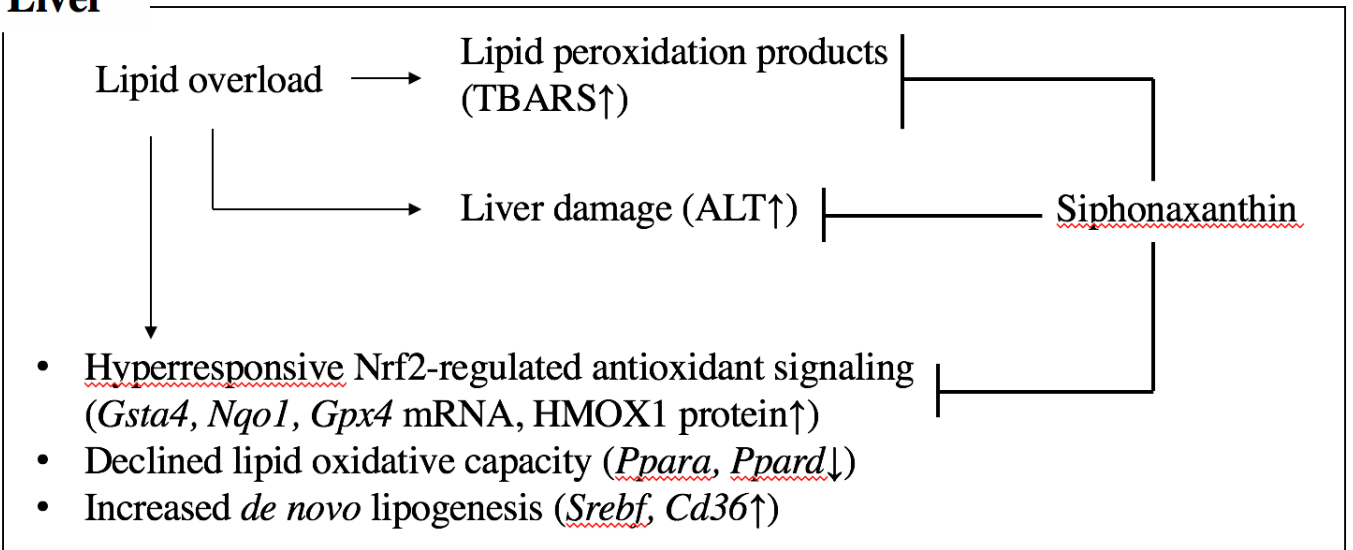


Fig. 8

Liver



Kidney

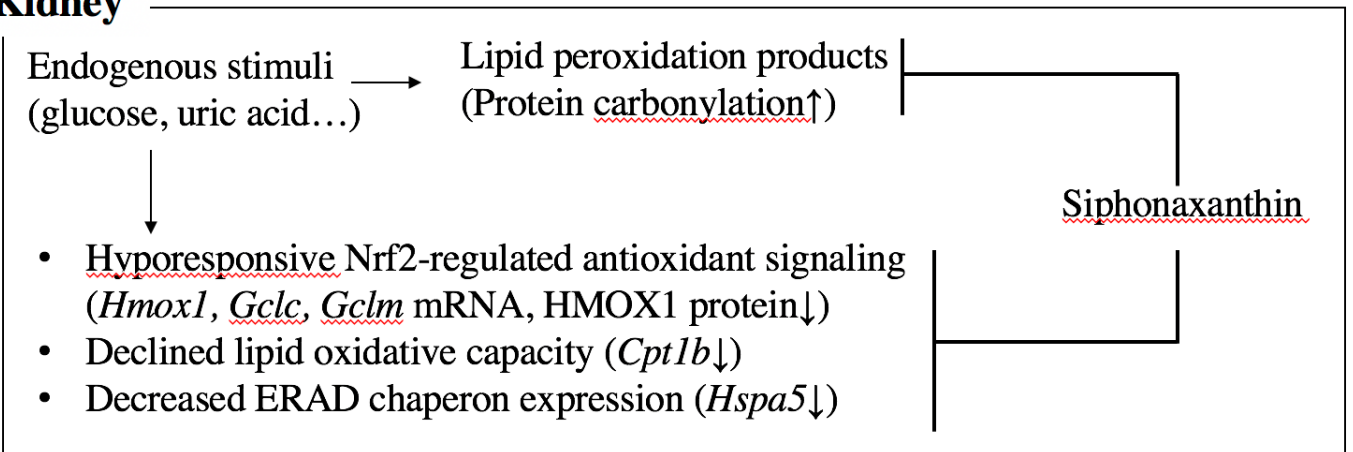


Table 1 Diet Ingredients of the diets (g/Kg)

	Basal AIN 93 G diet	HFD	SPX diet
Milk Casein	200	228.07	228.07
L-Cystine	3	3.42	3.42
Corn Starch	397.486	83.01	83.01
α -Corn Starch	132		
Maltodextrin 10		114.03	114.03
Sucrose	100	197.04	197.04
Cellulose	50	57.01	57.01
Soybean Oil	70	50.04	49.88
Lard		202.40	202.40
Mineral Mix	35	11.40	11.4
DiCalcium Phosphate		14.82	14.82
Calcium Carbonate		6.27	6.27
Potassium Citrate, 1 H ₂ O		18.81	18.81
Vitamin Mix	10	11.40	11.40
Choline Bitartrate	2.5	2.28	2.28
Tert-Butylhydroquinone	0.014		
Siphonaxanthin	0	0	0.16
Total	1000	1000	1000

HFD, high-fat diet; SPX, high-fat diet + siphonaxanthin (0.016%, w/w).

Table 2 Human primers for quantitative real-time RT-PCR

Gene name	Primer sequence (5' > 3')	Primer sequence (3' > 5')
β -ACTIN	CATGTACGTTGCTATCCAGGC	CTCCTTAATGTCACGCACGAT
HMOX1	AAGACTGCGTTCCTGCTCAAC	AAAGCCCTACAGCAACTGTCTG
NQO1	ATGTATGACAAAGGACCCTTCC	TCCCTTGCAGAGAGTACATTGG
GSTA4	TTGGTACAGACCCGAAGCATT	CAGGGTTCTCTCCTTGAGGTT
GCLM	CATTTACAGCCTTACTGGGAGG	ATGCAGTCAAATCTGGTGGCA
GCLC	GGAGACCAGAGTATGGGAGTT	CCGGCGTTTTTCGCATGTTG
GPX4	GAGGCAAGACCGAAGTAAACTAC	CCGAACTGGTTACACGGGAA
SOD2	GCTCCGGTTTTGGGGTATCTG	GCGTTGATGTGAGGTTCCAG

Table 3 Mouse primers quantitative real-time RT-PCR

Gene name	Primer sequence (5' > 3')	Primer sequence (3' > 5')
β -actin	CCTCTATGCCAACACAGTGC	GTACTTGCGCTCAGGAGGAG
Nqo1	AGAGAGTGCTCGTAGCAGGAT	GTGGTGATAGAAAGCAAGGTCTT
Gsta4	AGCTCAGTTGGGCAGACATC	TCCTGACCACCTCAACATAGG
Hmox1	GATAGAGCGCAACAAGCAGAA	CAGTGAGGCCCATACCAGAAG
Sod1	AACCAGTTGTGTTGTCAGGAC	CCACCATGTTTTCTTAGAGTGAGG
Sod2	CAGACCTGCCTTACGACTATGG	CTCGGTGGCGTTGAGATTGTT
Sod3	CCTTCTTGTTCTACGGCTTGC	TCGCCTATCTTCTCAACCAGG
Gpx1	AGTCCACCGTGTATGCCTTCT	GAGACGCGACATTCTCAATGA
Gpx4	TGTGCATCCCGCGATGATT	CCCTGTACTTATCCAGGCAGA
Gclc	GGCTACTTCTGTACTAGGAGAGC	TGCCGGATGTTTCTTGTTAGAG
Gelm	CTTCGCCTCCGATTGAAGATG	AAAGGCAGTCAAATCTGGTGG
Srebfl	GGAGCCATGGATTGCACATT	GCTTCCAGAGAGGAGCCAG
Acacb	CGCTCACCAACAGTAAGGTGG	GCTTGGCAGGGAGTTCCTC
Cd36	ATGGGCTGTGATCGGAACTG	TTTGCCACGTCATCTGGGTTT
Slc2a4	GTGACTGGAACACTGGTCCTA	CCAGCCACGTTGCATTGTAG
Acox1	TAACTTCCTCACTCGAAGCCA	AGTTCCATGACCCATCTCTGTC
Cpt1a	CTCCGCCTGAGCCATGAAG	CACCAGTGATGATGCCATTCT
Cpt1b	TTGCCCTACAGCTGGCTCATTTCC	GCACCCAGATGATTGGGATACTGT
Ppara	TACTGCCGTTTTTACAAGTGC	AGGTCGTGTTTACAGGTAAGA
Ppard	AATGCGCTGGAGCTCGATGAC	ACTGGCTGTCAGGGTGGTTG
Atf3	GAGGATTTTGCTAACCTGACACC	TTGACGGTAACTGACTCCAGC
Atf4	AAGGAGGAAGACACTCCCTCT	CAGGTGGGTCATAAGGTTTGG
Atf6	TCGCCTTTTAGTCCGGTTCTT	GGCTCCATAGGTCTGACTCC
Xbp1	AGCAGCAAGTGGTGGATTTG	GAGTTTTTCTCCCGTAAAAGCTGA
Hspa5	GCATCACGCCGTCGTATGT	ATTCCAAGTGCGTCCGATGAG

Table 4 Body and tissue weight, food intake

	Normal	Control	SPX
Final body weight (g)	32.0±1.09 ^a	55.3±1.36 ^b	54.7±1.07 ^b
Δ body weight (g)	9.28±1.15 ^a	16.0±0.30 ^b	16.5±0.78 ^b
Food intake (g/day/mouse)	3.04±0.20	3.30±0.05	3.33±0.07
Liver weight (mg/g body weight)	3.78±0.11 ^a	7.08±0.42 ^b	6.38±0.21 ^b
BAT (mg/g body weight)	0.18±0.05	0.06±0.01	0.06±0.01
Mesenteric WAT (mg/g body weight)	1.90±0.13 ^a	3.90±0.05 ^b	3.70±0.09 ^b
Perirenal WAT (mg/g body weight)	1.62±0.19 ^a	4.70±0.37 ^b	5.07±0.20 ^b
Epididymal WAT (mg/g body weight)	3.70±0.38 ^a	7.43±0.58 ^b	7.08±0.43 ^b

Values are mean ± SEM (n=6 for normal and SPX group, n=3 for control group). Values in a row not sharing a common letter differ significantly (p<0.05). Normal, lean mice fed on a basal AIN 93 G diet; Control, obese mice fed on a HFD; SPX, obese mice fed on a HFD supplemented with siphonaxanthin; BAT, brown adipose tissue; WAT, white adipose tissue.

Table 5 Plasma physiological measurements

	Normal	Control	SPX
Glucose (mg/dL)	273±10.1 ^a	407±8.58 ^b	331±22.2 ^{a,b}
Triacylglycerol (mg/dL)	73.5±12.3	61.0±6.87	68.4±7.51
Free cholesterol ((mg/dL)	29.8±0.52 ^a	82.9±8.30 ^b	87.6±5.82 ^b
HDL cholesterol (mg/dL)	85.0±2.14 ^a	156±6.57 ^b	166±7.84 ^b
Total cholesterol (mg/dL)	123±3.27 ^a	264±17.1 ^b	273±13.9 ^b
NEFA (mEq/L)	0.54±0.09	0.74±0.03	0.73±0.02
ALT (UI/L)	7.47±0.46 ^a	157±16.0 ^c	89.8±16.5 ^b
AST (UI/L)	11.9±0.43 ^a	228±40.8 ^b	164±35.2 ^b
Creatinine (mg/dl)	0.76±0.03	0.82±0.09	0.89±0.06

Values are mean ± SEM (n=6 for normal and SPX group, n=3 for control group). Values in a row not sharing a common letter differ significantly (p<0.05). Normal, lean mice fed on basal AIN 93 G diet; Control, obese mice fed on a HFD; SPX, obese mice fed on a HFD supplemented with siphonaxanthin; NEFA, non-esterified fatty acid; ALT, alanine transaminase; AST, aspartate transaminase.

Table 6 Liver lipid measurements

	Normal	Control	SPX
Triacylglycerol (mg/g tissue)	33.1±5.26 ^a	185±4.20 ^b	190±5.41 ^b
Total cholesterol (mg/g tissue)	1.98±0.09 ^a	6.32±0.24 ^b	5.41±0.34 ^b
NEFA (μEq/g)	7.50±1.20	7.60±0.70	8.90±1.00

Values are mean ± SEM (n=6 for normal and SPX group, n=3 for control group). Values in a row not sharing a common letter differ significantly (p<0.05). Normal, lean mice fed on basal AIN93G diet; Control, obese mice fed on a HFD; SPX, obese mice fed on a HFD supplemented with siphonaxanthin; NEFA, non-esterified fatty acid;